On the use of optical probes to monitor the thermal transitions in spin-coated poly(9,9-dioctylfluorene) films

2005 J. Phys.: Condens. Matter 17 6307

(http://iopscience.iop.org/0953-8984/17/41/002)

INSTITUTE OF PHYSICS PUBLISHING JOURNAL OF PHYSICS: CONDENSED MATTER

J. Phys.: Condens. Matter **17** (2005) 6307–6318 doi:10.1088/0953-8984/17/41/002

On the use of optical probes to monitor the thermal transitions in spin-coated poly(9,9-dioctylfluorene) films*

M Sims[1], K Zheng[1], M Campoy Quiles[1], R Xia[1], P N Stavrinou[1], D D C Bradley[1,3] and P Etchegoin[2]

[1] Experimental Solid State Group, Department of Physics, Imperial College London, Prince Consort Road, London SW7 2BW, UK
[2] The McDiarmid Institute for Advanced Materials and Nanotechnology, School of Chemical and Physical Sciences, Victoria University of Wellington, PO Box 600, Wellington, New Zealand

E-mail: D.Bradley@imperial.ac.uk

Received 20 May 2005, in final form 27 July 2005
Published 30 September 2005
Online at stacks.iop.org/JPhysCM/17/6307

Abstract

We report on the use of optical probes to determine the thermal transition temperatures of spin-coated films of the prototypical fluorene based conjugated polymer poly(9,9-dioctylfluorene) (PFO). In particular we focus here on the use of temperature dependent photoluminescence (PL) measurements that are well suited to the study of PFO and other intrinsically fluorescent polymers and blends. The integrated PL intensity reveals clear signatures of the glass transition temperature (T_g), the onset of crystallization (T_c) and subsequent melting into the nematic liquid crystalline mesophase (T_m). The PL intensity determined transitions are shown to be consistent with an independent optical probe, namely spectroscopic ellipsometry, and with differential scanning calorimetry measurements on bulk samples. The especially strong contrast in PL intensity at T_c and T_m is shown to be a consequence of changes in light out-coupling in the direction of PL detection, a conclusion that is confirmed by measurements of edge emitted waveguided PL and amplified spontaneous emission, and by analysis of ellipsometry data.

As 'soft solids' with characteristically weak inter-molecular interactions, polymers have the ability to adopt a wide variety of different physical structures, the control of which provides a desirable means to tune functional properties. Thermal transitions between physical structures are of strong interest because thermal processing can be convenient but also because the

* Based on a presentation to the American Physical Society March Meeting 2005.
[3] Author to whom any correspondence should be addressed.

unintentional occurrence of transitions due to changes in ambient temperature represents an important source of potential instability. Conjugated polymers represent one class of polymer that is of strong current interest for application: electroluminescent displays, lighting, radio frequency identification tags, driver circuits for liquid crystal and electrophoretic displays, solar cells, light sources and detectors for microanalysis systems, lasers, amplifiers and optical switches are all under development. The family of fluorene-based polymers has further proven to be one of the leading materials sets in this class and poly(9,9-dioctylfluorene) (PFO), the subject of the study reported here, is a prototype for this family. The focus of the present work is to establish the utility of optical probes to monitor the thermal transition temperatures for thin film samples, typical of those used in device structures. In particular, we focus on the use of temperature dependent photoluminescence (PL) measurements that are well suited to the study of intrinsically fluorescent polymers and blends. We explore the nature of the PL contrast that allows detection of thermal transitions in PFO. We also demonstrate the consistency of the PL determined transition temperatures with those derived from another optical measurement, namely spectroscopic ellipsometry, and with differential scanning calorimetry measurements on bulk samples.

PFO films deposited from solution start off in a non-equilibrium glassy state, first reached when the glass transition temperature of the polymer/solvent system rises (on solvent loss) above ambient temperature. On heating [1, 2], glassy films pass into a rubbery state at the glass transition temperature, T_g, and the resulting increase in allowed molecular motions gives rise to the necessary geometric relaxation for crystallization to occur at T_c. Further heating leads to a melting transition at T_m above which a nematic liquid crystalline mesophase is formed. At higher temperatures still, the nematic liquid crystal clears into an isotropic melt at T_{iso}. Slow cooling from the isotropic or liquid crystalline melts recovers the crystalline phase, though with evidence that there is a slightly modified crystal structure on cooling. The crystalline phase is retained on cooling to room temperature. Alternatively, rapid cooling from the isotropic or liquid crystalline melts to below T_g allows the film to be quenched into a glassy state, different from the original glass formed during deposition from solution. One may thermally cycle between these different structural phases, with the exception that the initial spin-coated glass structure can never be recovered after heating above T_g. PFO represents an excellent choice with which to explore the use of PL as an optical probe to monitor thermal transitions in conjugated polymers: it displays a wide range of physical structures between which a sample may be thermally cycled and it possesses a strong PL emission within each of them [2].

PFO has other interesting features, especially its ability to be uniaxially oriented in its nematic liquid crystalline mesophase [1, 3–7] and its ability to adopt a well defined, extended, rigid chain conformation, samples containing a fraction of which are termed β-phase samples [3, 4, 8–14]. Liquid crystalline orientation on suitable alignment layers (e.g. rubbed polyimide) allows the preparation of monodomain samples with high degrees of order, a first for so-called 'hairy rod' liquid crystal polymers [1, 3–7]. These in turn provide highly polarized light emission [1, 3, 5–7], enhanced charge transport [15], and a large optical birefringence [6, 16]. The β-phase conformation can be induced in a number of ways and its presence is readily detected since it possesses distinct, red shifted spectral features that are straightforwardly deconvoluted: there is a step change, not a gradual shift in spectra when the β-phase conformation is adopted [3, 4, 8–14]. The β-phase conformation is characterized by exceptionally well resolved PL spectra that allow detailed studies of vibronic coupling and excitation dynamics [9, 10, 12–14]. β-phase samples further represent a novel 'self-doped' donor–acceptor (D–A) system in which to study energy transfer processes [9, 10, 12–14]. The uniqueness of the β-phase conformation is supported by a recent detailed modelling study in

which a compact, chain extended conformation with the octyl side-chains folded back and lying alongside a helical backbone has been identified [13]. From a practical perspective, the β-phase conformation, when isolated in an inert polymer matrix, offers enhanced optical gain properties via both an extended spectral range and an increased stimulated emission magnitude [11]. It further offers novel ultrafast optical gain switching behaviour in the same matrix isolated environment [11]. Finally, β-phase chains induced within oriented liquid crystalline glass films provide a significant enhancement in the PL emission polarization ratio [3]. We will not consider oriented liquid crystalline and β-phase samples further in this study: they are, however, clearly of interest for future study in respect of using optical methods to probe their thermal transition behaviours.

Poly(9,9-dioctylfluorene), with a typical degree of polymerization $n \approx 100$, was synthesized by The Dow Chemical Company [17] and was subjected to a rigorous clean-up before shipping: the polymer was used as received. For PL and absorption experiments, PFO films were prepared by spin-coating onto Spectrosil B fused silica substrates from a 20 mg ml^{-1} chloroform (HPLC grade) solution at a spin speed of 3000 rpm. This resulted in films of thickness $\sim$200 nm with no detectable β-phase emission. For PL and absorption measurements the samples were held *in vacuo* ($\sim 10^{-6}$ mbar) within a home-built hot stage. PL was excited at $\sim$380 nm by normal incidence exposure to a monochromated Bentham xenon lamp, the emission collected, after passing through the sample, with a silica fibre bundle held at $\sim$45° to normal incidence, spectrally dispersed with a spectrograph and detected with an Instaspec IV cooled charge-coupled device (CCD). All spectra were corrected for the power response of the detection system. The experiments were conducted using a home-built, automated shuttering system that opened a shutter placed in the excitation path at each of a set of predetermined temperatures: 2 °C temperature intervals were used, monitored by a thermocouple attached to the sample heating block. The shutter was typically held open for 1–2 s periods (during which time the CCD signal was integrated) and then closed so that the samples were kept in the dark at all other times. A heating rate of 1 °C min^{-1} was selected to ensure that thermal equilibrium was reached at each PL measurement temperature. The use of the shuttering system ensured that photodegradation was kept to a minimum (undetectable) during these lengthy experiments: continuous exposure to UV at elevated temperature can otherwise lead to the formation of fluorenone moieties and the consequent appearance of their red-shifted excimer emission (the so-called 'g-band') [18, 19]. The adoption of a shuttering system allowed us to cycle our samples over extended temperature ranges without the appearance of any g-band emission. Absorption spectra were measured with a Unicam IV, UV/vis spectrophotometer into which the home-built hot stage was inserted.

In order to better understand the nature of the strong PL intensity contrast (*vide infra*) observed on heating PFO films into their crystalline phase ($T_c < T < T_m$) we have also measured photoluminescence quantum efficiencies (PLQEs), monitored changes in the spectrum of the PL emitted from the substrate edge (light waveguided parallel to the substrate plane) and undertaken stripe-pump amplified spontaneous emission (ASE) measurements of in-plane optical gain and loss. For PLQE measurements, PFO films spin coated on Spectrosil B substrates were placed within a calibrated integrating sphere. PL was again excited by exposure to $\sim$380 nm light from a monochromated xenon lamp: a fixed fraction of this PL emission was collected via an optic fibre link, dispersed in a spectrograph, and detected with an Instaspec IV CCD. A comparison of the input and output intensities then allows absolute determination of the quantum efficiency [2]. PLQE measurements were performed at room temperature only: our PLQE apparatus does not allow temperature dependent measurements.

For sample-edge-detected PL experiments, the silica fibre bundle used to collect the emission light was held in the substrate plane and positioned with its tip a distance 1–2 mm

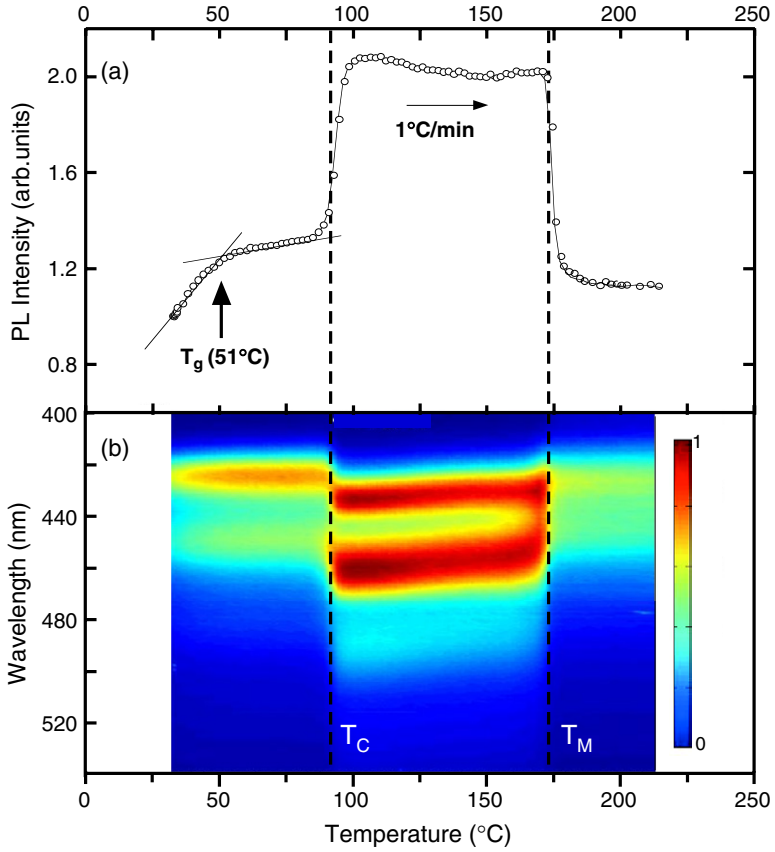

Figure 1. Temperature dependent photoluminescence (PL) data for a PFO thin film during heating from room temperature at a rate of 1 °C min^{-1}: (a) spectrally integrated, forward emitted, PL intensity (see text for details of experimental geometry). Data are normalized to the room temperature value. (b) False colour intensity plot showing the corresponding spectral evolution during heating. The dashed vertical lines in (a) and (b) locate the crystallization temperature, T_c, and the temperature, T_m, at which the sample melts into a nematic liquid crystal phase.

away from the substrate edge. The latter measurements were performed in air and at room temperature. Stripe-pumped ASE measurements [20] were also performed in air at room temperature on spin-coated (glassy) films of thickness ∼120 nm and on the same samples after crystallization (heating above T_c) and rapid cooling back to room temperature. A Q-switched, neodymium ion doped yttrium aluminium garnet (Nd^{3+}:YAG) laser pumped, type-II β-BaB_2O_4 (BBO) optical parametric oscillator that delivered 10 ns pulses at a repetition rate of 10 Hz was used here as the excitation source. As for the PL and PLQE measurements, the excitation wavelength was chosen to be 380 nm to coincide with the peak of the long wavelength UV–vis absorption band. The pulse energy incident on the sample was adjusted by the insertion of calibrated neutral density filters into the beam path. The pump beam was focused with a cylindrical lens and spatially filtered through an adjustable slit to create a narrow 400 μm × 4 mm excitation stripe on the sample. At sufficient excitation intensity, the spontaneously emitted photons that are waveguided along the stripe-shaped gain region are amplified via stimulated emission. This results in most of the light being emitted from the ends of the stripe with a characteristically gain narrowed spectrum and strongly directional

emission. One end of the pump stripe was placed at the edge of the film and the emission collected and detected with the same fibre bundle, spectrograph and CCD combination as used for PL measurements. Loss measurements involved monitoring the ASE intensity whilst gradually translating the pump stripe away from the sample edge [20]. Since the emission from the end of the (fixed length) pump stripe can be assumed to have constant intensity, I_0, the emission from the edge of the sample should decrease as a result of the waveguide losses (absorption and scattering of radiation out of the guide) that occur during propagation across the unpumped region. The detected output intensity, I_{out}, can be expressed as

$$I_{\text{out}} = I_0 \exp(-\alpha x)$$

where x is the length of the unpumped region between the end of the stripe and the edge of the sample and α is a combined waveguide loss coefficient.

Ellipsometry measurements were performed on a 108 nm thickness PFO sample spin coated (2000 rpm, 40 s) from a 15 mg ml^{-1} (HPLC grade) toluene solution onto a Spectrosil B fused silica substrate. These films showed no evidence for a β-phase component and the data obtained are thus fully comparable with the data obtained for the samples spin coated from chloroform. To avoid oxidation during annealing, the sample was placed inside a SOPRA supplied vacuum chamber (5×10^{-7} mbar) equipped with a temperature controlled sample holder. The temperature was varied from 25 to 140 °C at a rate of 1 °C min^{-1} using a Lakeshore 331 temperature controller. Spectroscopic ellipsometry scans were recorded at 10 °C temperature intervals using a SOPRA GESP 5 reflection mode rotating polarizer ellipsometer. The data were recorded for an incidence angle of 60° with respect to the substrate normal (close to the Brewster angle of the Spectrosil substrate), across a wavelength range from 250 to 850 nm (5 nm steps). The sample was allowed to equilibrate for 25 min at each temperature before measurement.

Isotropic fits were used to analyse the ellipsometric data. As a consequence, the deduced optical constants are expected to be a good approximation to the in-plane index ($n_{\text{in-plane}}$) of the film [16, 21]. Following a previous study [22] we have used three exciton (zero-dimension critical point) lineshapes to model the dielectric function of PFO. The film thickness was also used as a fitting parameter. Good agreement was found between the ellipsometrically deduced film thickness and profilometry (Alpha Step) measurements performed on the same sample, at room temperature. The resulting standard deviation (σ) between the modelled (for Spectrosil substrate plus a 108 nm thick PFO film) and experimentally determined ellipsometry data was $\sim 1.3 \times 10^{-3}$ at or near room temperature. However, for the same model, σ was found to almost double for temperatures $T > T_c$. It was then necessary to introduce a depolarization element, modelled as a roughness layer on top of the polymer thin film, in order to return σ to its initially low value. This layer was taken to comprise a fraction $(30 \pm 2)\%$ of polymer in air, with its dielectric function described via the Bruggeman model. In agreement with the proposed origin of the PL contrast (*vide infra*), the addition of a roughness layer approximates well to an onset of scattering that will tend to depolarize the incident light.

Figure 1 shows the evolution of (a) the integrated PL intensity and (b) the PL spectrum (in the form of a false colour intensity contour plot) for a pristine, $\sim$ 200 nm thickness, spin-coated PFO film on heating (1 °C min^{-1}) from room temperature to 220 °C. This is a typical data set for a film prepared so as to avoid the presence of a β-phase component. In figure 1(b) the light intensity (z-axis) increases from blue to red, as indicated by the scale bar to the right of the figure. Vertical slices through this contour plot, defined by the (z, y) i.e. (intensity, wavelength) plane, correspond to PL spectra recorded at specific temperatures: examples are shown in figure 2 at 30, 115 and 180 °C. These temperatures are characteristic of the spin-coated (glassy), crystalline and liquid crystalline phases respectively. The absence of a g-band

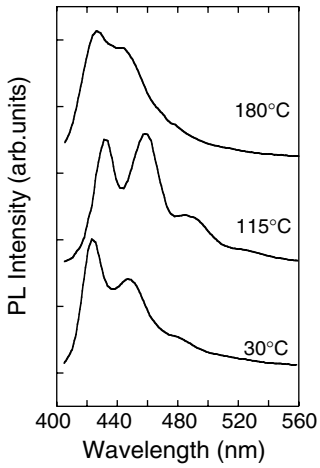

Figure 2. Representative PFO thin film PL spectra recorded below T_c (at 30 °C), between T_c and T_m (at 115 °C) and above T_m (at 180 °C). These spectra correspond to (intensity, wavelength) slices through the data presented in figure 1(b). They are normalized and offset for clarity and the experimental measurement details are given in the text.

emission component, expected to peak at 535 nm [18], attests to the efficacy of the shuttered exposure, *in vacuo* measurement procedure in preventing photo-oxidation. It is also clear that no resolved β-phase emission, with characteristic 0–0 vibronic peak at 440 nm [9, 10], is seen in the pristine spin-coated film (30 °C spectrum).

Owing to rapid solvent evaporation during the spin-coating process and the arrest of geometric relaxation on passing into a glassy state, the resulting films can be considered at room temperature to be relatively heterogeneous and consequently to possess a less than optimally packed structure. There is a tendency to orient in the plane of the substrate but otherwise the films are rather disordered [16]. Viewed from a direction normal to the substrate plane the films appear isotropic and they are characterized by an inhomogeneously broadened π–π^* absorption band centred at ∼384 nm with a typical optical absorption coefficient $\alpha = 2.8 \times 10^5$ cm^{-1}.

The effect of heating can best be described by separating the PL data in figures 1(a) and (b) into three temperature regions, delineated by the two vertical dashed lines. These lie at $T = 93$ and 173 °C, at which temperatures the PL spectra are seen to abruptly change (see figure 1(b)), first showing a step-like red shift then a step-like blue shift. Moving from left to right (low to high temperature), the PL in the first region (30 °C $< T <$ 90 °C) has a spectrum that remains largely unchanged from that of the pristine spin coated film, except that some additional line broadening occurs on heating (clearly seen in figure 1(b)). Two vibronic peaks (effective 0–0 and 0–1) are observed at ∼424 and ∼449 nm, with a weak shoulder (effective 0–2) near 480 nm. The PL intensity on the other hand rises non-linearly with a clear change in thermal gradient at 51 °C. This break point identifies the glass transition temperature. Its value is consistent with differential scanning calorimetry data, measured for a bulk PFO powder sample using a heating rate of 20 °C min^{-1} [1] and with ellipsometrically measured tan $\psi(T)$ data [23]. The observed behaviour is very much as reported for non-conjugated (saturated) polymer samples doped with dyes (to provide the necessary PL emission) [24]. This confirms the utility of a PL optical probe to measure the glass transition temperature for light emitting conjugated polymers. Importantly, unlike the case of most saturated polymers that do not have efficient intrinsic photoluminescence, there is no need here to disperse a separate fluorophore

within the polymer film as a probe molecule. This means that there is correspondingly no concern that the PL monitored transitions are modified in any way by the requirements of the experiment. In terms of absorption spectra there is little change within this temperature region: the optical density drops by ∼2% and there is a slight broadening of the lineshape.

The second temperature region (90 °C $< T <$ 170 °C) is delineated by two step-like changes in PL intensity, with first a factor of 1.58 increase at $T \sim 90$ °C and then a factor of 1.78 decrease at $T \sim 170$ °C. The first, upward step identifies the crystallization temperature and, as for T_g, its value is consistent with differential scanning calorimetry data [1] which showed an exothermic crystallization peak at 93 °C. There are correspondingly abrupt spectral changes in PL (see figures 1(b) and 2) consistent with previously reported room temperature measurements on films crystallized by slow cooling from the melt [2]. The PL spectrum markedly red-shifts and the higher order vibronic peaks increase in magnitude relative to the 0–0 peak. At 115 °C (figure 2) there are clearly resolved vibronic peaks at 432 (0–0), 459 (0–1) and 490 nm (0–2), with a weaker feature at 526 nm (0–3): the strongest vibronic peak is now the 0–1 rather than the 0–0 that is strongest for the spin-coated glassy film at 30 °C. The absorption spectrum does not change very dramatically. The long wavelength peak absorption coefficient decreases by ∼8% to $\alpha = 2.58 \times 10^5$ cm^{-1}, but the spectrum as a whole broadens slightly and the integrated absorption in fact increases by 5%. The absorption edge starts to show some evidence of vibronic structure although it is not very pronounced. The suppression of the 0–0 vibronic peak in the PL spectrum relative to the 0–1 peak may then, at least in part, be the consequence of an increased self-absorption. We would note further that, even without a substantial change in the absorption spectrum, the degree of self-absorption might significantly increase. This will be the case, for instance, whenever the path length travelled by the emission before it reaches the detector significantly increases. As we discuss below, there are circumstances in which this scenario might well apply.

An important question to answer is why the measured PL intensity almost doubles on crystallization. The mechanism responsible clearly provides excellent contrast with which to detect the transition temperature but does it also indicate an absolute improvement in emission properties? Photoluminescence quantum efficiency (PLQE) measurements were carried out at room temperature in an integrating sphere to address this question. We found PLQE ∼0.57 for spin-coated samples, whilst following crystallization (heating to a temperature T in the range $T_c < T < T_m$) and cooling rapidly to room temperature we found PLQE ∼ 0.63. The moderate increase (≈10%) is consistent with earlier reports [2] but clearly shows that another effect must be responsible for the majority of the observed change in PL intensity.

A re-direction of emission into the forward hemisphere, thus increasing the intensity incident on the detector held at $\theta \approx 45°$ to the sample normal, appears the most likely explanation. To investigate this further we have undertaken a series of additional optical characterizations. Thin films of conjugated polymer spin-coated on Spectrosil B substrates often behave as slab waveguides with a significant fraction of light propagating in the plane and emitted from the edge of the substrate [25, 26]. This can be an important issue for polymer light emitting diodes as it will limit the forward emitted (useful) intensity [25, 26]. Such a situation was found to be the case here where our spin-coated films showed strong substrate edge emission with a PL spectrum modulated by waveguiding: the corresponding spectrum is shown in figure 3(a) (lower curve). The dominant feature peaked at ∼430 nm corresponds to light propagation within a characteristic mode of the slab waveguide. After crystallization (and cooling to room temperature) the edge emitted PL was strongly reduced in magnitude and its spectrum once again showed the expected vibronic structure with no clear signature of waveguide mode modulation: the corresponding spectrum is shown in figure 3(a) (upper curve). On the basis of this evidence we considered that the step change in the integrated PL intensity

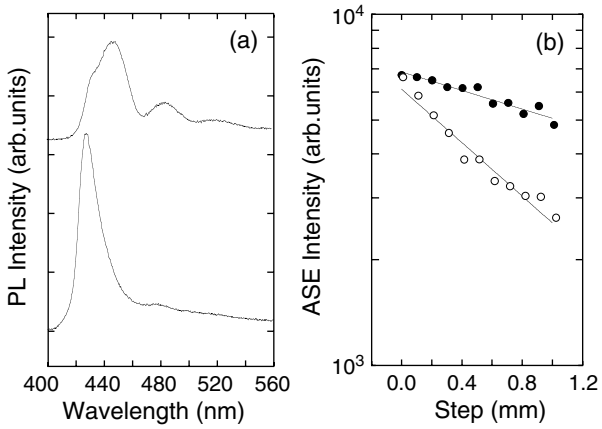

Figure 3. (a) Substrate edge detected PL spectra for a 205 nm thickness, spin-coated glassy PFO film (lower curve) and an initially identical film that had been subsequently crystallized at 125 °C for 5 min, and then rapidly quenched to room temperature (upper curve). (b) Amplified spontaneous emission intensity for a 120 nm PFO film as a function of pump-stripe displacement away from the edge of the substrate (see the text for experimental details). Filled circles represent the data collected for an as-spin-coated glassy film, whilst open circles are the corresponding data for an initially identical film that had been subsequently crystallized at 125 °C for 5 min, and then rapidly quenched to room temperature. The straight-line fits to the data allow an effective (exponential) loss coefficient to be determined.

at T_c resulted from scattering within the film plane. Scattering frustrates in-plane waveguiding and forces more of the PL to be emitted in the forward direction (towards the detector). This may not be simply the consequence of a heterogeneous nucleation and growth of crystalline domains since x-ray studies indicate crystallite sizes only of order 15–50 nm, albeit for fibre samples [4]. Larger periodicities would be expected to be necessary for efficient scattering at the PL emission wavelengths, indicating the likely existence of longer-range structure/surface modulation (cf discussion of ellipsometry data below).

Amplified spontaneous emission (ASE) experiments allowed us to confirm the validity of this proposal: using the stripe pump geometry, the build-up of ASE occurs via in-plane waveguiding along the stripe's principal axis. ASE gain and loss measurements performed on spin-coated glass and crystalline PFO films showed that, as expected from above, crystallization has a deleterious effect on ASE, decreasing the gain and increasing the loss (see figure 3(b)). A loss coefficient, $\alpha = 3.0\ \mathrm{cm}^{-1}$, was deduced for the spin-coated glassy film, in agreement with previous ASE studies [20]. Samples heated to 125 °C and held there for 5 min to crystallize before quenching to room temperature had a strongly increased loss coefficient, namely $\alpha = 8.8\ \mathrm{cm}^{-1}$ entirely consistent with the proposed increase in scattering.

The downward step in PL intensity (figure 1(a)) at $T \sim 170$ °C identifies the melt temperature at which the film enters its nematic liquid crystalline mesophase. As for T_g and T_c, the deduced T_m value is consistent with differential scanning calorimetry data [1] which showed an endothermic melting peak at $T \sim 160$ °C, just slightly lower in temperature than the down step here in PL intensity. There is again a correspondingly abrupt change in the PL spectrum (see figures 1(b) and 2) with an evident blue shift and a washing out of vibronic structure. The PL spectrum presented here for the nematic mesophase, measured at 180 °C (figure 2), shows a peak at 426 nm (0–0), with a poorly resolved shoulder at 444 nm (0–1). The vibronic peak structure is significantly restored and the spectrum also red shifts when the sample is rapidly quenched into the nematic glass state [2]. This behaviour is quite reasonable given

the expected increase in segmental motion, and consequent reduction in conformationally controlled π-electron delocalization length (conjugation length), that will occur at elevated temperatures. Interestingly, the strong increase in inhomogeneous broadening (smearing of vibronic structure) starts to occur at ~155–160 °C: figure 1(b) shows a merging of the strong 0–0 and 0–1 vibronic peaks of the crystalline sample at this temperature. The broadening thus occurs at a temperature closer to the melt endotherm measured in differential scanning calorimetry whilst the down step in PL intensity more closely matches the temperature at which a birefringent (nematic) fluid is first observed when the sample is viewed sandwiched between crossed polarizers in an optical microscope [1]. The absorption spectrum changes more abruptly here with a strong flattening of the long wavelength absorption peak and a better resolution of vibronic structure.

The down-step in PL intensity is understood again not to be the consequence of a change in PLQE but rather the effect of a reduction in scattering upon entering the nematic liquid crystalline state. As a result in-plane waveguiding becomes easier again and less light propagates in the forward direction, reducing the measured PL intensity. Quenching into a nematic glass by rapid cooling to room temperature provides films that are well suited to the observation of ASE and indeed, due to their birefringence, oriented nematic glass films offer additional optical confinement, leading to enhanced gain properties [25]. Such quenched nematic glass films were measured here to have a PLQE = 0.75, again consistent with earlier studies [2], where a value of 0.78 was reported. This is clearly *larger* than the room temperature value found for the crystalline films and hence completely inconsistent with a PLQE related explanation for the down step in PL intensity.

In support of the PL measurements we have used spectroscopic ellipsometry as a complementary optical probe. Ellipsometry represents a more established tool in the study of polymer thermal transitions [27–32] and one that does not rely on PL emission as a contrast mechanism. It can thus be used to provide an independent validation of the utility of temperature dependent PL intensity data to monitor the thermal transitions. It also allows confirmation (*vide infra*) of the proposed dominance of scattering in delineating the PL intensity within the crystalline phase from that within both glassy and liquid crystalline phases. Modelling of ellipsometric data allows determination of the film thickness and the spectral dispersion of the complex refractive index. Thus, if data are collected as a function of temperature, one can map the way in which these parameters vary. Here, we have used an isotropic model for the PFO film (see experimental section) to deduce the optical constants and film thickness. These data are presented in figure 4. Figure 4(a) displays the temperature variation of the refractive index, n, at 466 nm, namely a wavelength well separated from the absorption edge but still within the PL emission window. The temperature variation of n shows a clear correlation with the PL intensity data shown in figure 1, with a step up in n at T_c and a step down in n at T_m. The transition temperatures are slightly lower than deduced from the PL intensity data: the step up in n occurs at 70–80 °C and the step down at 150–160 °C. One explanation for this difference is that it is a consequence of the rather different heating conditions for the two experiments, namely 1 °C min^{-1} continuous temperature ramp with 1–2 s measurement times for the PL intensity data *versus* discrete temperature steps ($\Delta T \sim 10$ °C) with 25 min equilibration times and 20 min measurement times for the ellipsometry data.

The corresponding film thickness variation with temperature, namely $d(T)$, is shown in figure 4(b). This has a reciprocal relationship with $n(T)$: when d decreases n increases and *vice versa*. Also shown in figure 4(c) is the thickness of a 'roughness layer' (see the experimental section) that had to be included in the model in order to achieve a satisfactory fit to the ellipsometry data over the temperature range 70 °C $\leqslant T \leqslant$ 160 °C. This layer causes a depolarization of the incident light and is thus essentially an approximation to the effect of

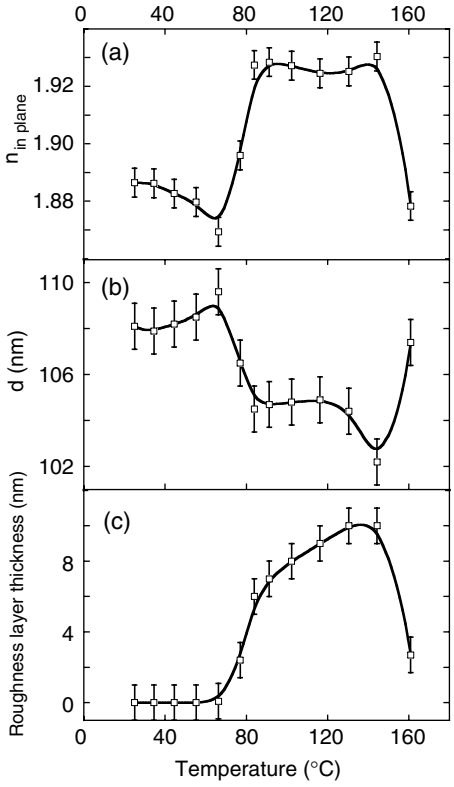

Figure 4. Temperature dependent film parameters extracted from the spectroscopic ellipsometry data recorded during heating of an initially (as-spin-coated) glassy PFO film. (a) Temperature variation of the deduced in-plane refractive index, $n_{\text{in-plane}}$. (b) Temperature variation of the deduced film thickness. (c) Temperature variation of the thickness of a roughness layer contribution that needed to be added to the model in order to satisfactorily fit the ellipsometry data over the temperature range $\sim 70\,^{\circ}\text{C} \leqslant T \leqslant \sim 160\,^{\circ}\text{C}$ (see the experimental section for details).

scattering. The roughness layer contribution is unnecessary in the glass/rubber state below T_c and again becomes unimportant at T_m, signifying the return to a more homogeneous structure in the liquid crystalline melt. Our explanation of the contrast seen in the PL intensity data of figure 1 is thus fully supported by the ellipsometry measurements.

Ellipsometry also adds the information that the film shrinks on heating above T_c before expanding again on approaching T_m. The thickness reduction is some 5%, a plausible outcome of the improvement in packing associated with the adoption of a crystalline structure. A simple analysis of the relative changes in thickness and refractive index is also revealing. We have previously shown [22] for PFO and poly(9,9-dihexylfluorene), a close analogue with hexyl instead of octyl side chains, that the ratio of oscillator strengths (proportional to transition dipole moments ($\langle\mu\rangle$) and inverse thicknesses) can be related to the resulting refractive indices far from the absorption edge (e.g. at $\lambda = 850$ nm) by the expression

$$\frac{\langle\mu\rangle_1}{\langle\mu\rangle_2}\frac{d_2}{d_1} \simeq \frac{n_1^2 - 1}{n_2^2 - 1}.$$

Considering the changes in thickness and refractive index upon crystallization of PFO, parametrized here by $d_1 = 109.6$ nm, $d_2 = 104.5$ nm, n_1 (850 nm) $= 1.72$, and n_2

(850 nm) = 1.75, we find that the ∼5% change in thickness is matched by a change of ∼5% in $\frac{n_1^2-1}{n_2^2-1}$. This implies that $\langle\mu\rangle_1 \approx \langle\mu\rangle_2$ applies here, or, in other words, that the increase in refractive index upon crystallization can be assigned as wholly due to the densification of the film. We note further that the increase in refractive index for the crystalline structure will tend to enhance the effects of scattering since it leads to a larger Δn at the crystallite/disordered polymer, crystallite/air and crystallite/Spectrosil interfaces.

Conclusion

We have demonstrated that a relatively simple photoluminescence measurement can be put to effective use as an optical probe for monitoring the thermal transitions in thin films of the conjugated polymer poly(9,9-dioctylfluorene). The strong contrast at T_c and T_m was proposed to be a consequence of changes in the out-coupling of emitted light in the forward (normal to surface) direction, caused by scattering effects (that arise following crystallization) on in-plane waveguiding. Edge emitted photoluminescence and amplified spontaneous emission measurements were found to be consistent with this interpretation, as was an analysis of spectroscopic ellipsometry data. The latter provided an important independent validation of our photoluminescence intensity monitoring method and added useful additional insights concerning changes in film thickness and refractive index. The scattering induced frustration of in-plane waveguiding is of potential benefit to light emitting diode operation and such effects might indeed play a role in the performance enhancements that have previously been reported for thermally annealed film structures.

Having established measurements of the temperature dependence of the PL intensity as a means to determine thermal transition temperatures for PFO thin films we consider that this technique could now be profitably extended to the study of other photoluminescent conjugated materials. We expect that it would be particularly useful in the study of materials under development for display, lighting and optical gain applications: by design these tend to have high photoluminescence quantum efficiencies. As an optical technique, it also offers the possibility to directly monitor the thermal transition temperatures of conjugated organic thin films within device structures. One subject of great interest is how the transition temperatures depend in these circumstances on confinement effects (film thickness/interactions with the environment). It is of further interest to seek to implement this method in a much more straightforward way (e.g. without spectral dispersion) that might then be compatible with routine measurements in a production environment.

Acknowledgments

We thank M Ariu, A J Campbell, and C Hill for their input to the early stages of this project and for helpful discussions. We further thank R B Fletcher, M Inbasekaran, and J J O'Brien of The Dow Chemical Company for providing the polymer used in our study. Finally, we acknowledge the financial support of the UK Engineering and Physical Sciences Research Council (grants GR/R9708, GR/R07172, and GR/R55078).

References

[1] Grell M, Bradley D D C, Inbasekaran M and Woo E P 1997 *Adv. Mater.* **9** 798–802
[2] Ariu M, Lidzey D G, Sims M, Cadby A J, Lane P A and Bradley D D C 2002 *J. Phys.: Condens. Matter* **14** 9975–86

[3] Grell M, Bradley D D C, Long X, Chamberlain T, Inbasekaran M, Woo E P and Soliman M 1998 *Acta Polym.* **49** 439–44
[4] Grell M, Bradley D D C, Ungar G, Hill J and Whitehead K 1999 *Macromolecules* **32** 5810–7
[5] Whitehead K S, Grell M, Bradley D D C, Jandke M and Strohriegl P 2000 *Appl. Phys. Lett.* **76** 2946–8
[6] Virgili T, Lidzey D G, Grell M, Walker S, Asimakis A and Bradley D D C 2001 *Chem. Phys. Lett.* **341** 219–24
[7] Liem H, Etchegoin P, Whitehead K S and Bradley D D C 2003 *Adv. Funct. Mater.* **13** 66–72
[8] Bradley D D C, Grell M, Long X, Mellor H, Grice A W, Inbasekaran M and Woo E P 1997 *Proc. SPIE* **3145** 254–9
[9] Cadby A J, Lane P A, Mellor H, Martin S J, Grell M, Giebeler C, Bradley D D C, Wohlgenannt M, An C and Vardeny Z V 2000 *Phys. Rev.* B **62** 15604–9
[10] Ariu M, Sims M, Rahn M D, Hill J, Fox A M, Lidzey D G, Oda M, Cabanillas-Gonzalez J and Bradley D D C 2003 *Phys. Rev.* B **67** 195333
[11] Virgili T, Marinotto D, Lanzani G and Bradley D D C 2005 *Appl. Phys. Lett.* **86** 091113
[12] Khan A L T, Sreearunothai P, Herz L M, Banach M J and Köhler A 2004 *Phys. Rev.* B **69** 085201
[13] Chunwaschirasiri W, Tanto B, Huber D L and Winokur M J 2005 *Phys. Rev. Lett.* **94** 107402
[14] Rothe C, King S M, Dias F and Monkman A P 2004 *Phys. Rev.* B **70** 195213
[15] Redecker M, Bradley D D C, Inbasekaran M and Woo E P 1998 *Appl. Phys. Lett.* **73** 1565–7
Redecker M, Bradley D D C, Inbasekaran M and Woo E P 1999 *Appl. Phys. Lett.* **74** 1400–2
[16] Campoy Quiles M, Etchegoin P and Bradley D D C 2005 *Phys. Rev.* B **72** 04520
[17] Bernius M, Inbasekaran M, Woo E, Wu W S and Wujkowski L 1999 *Proc. SPIE* **3621** 93–102
[18] Sims M, Bradley D D C, Ariu M, Koeberg M, Asimakis A, Grell M and Lidzey D G 2004 *Adv. Funct. Mater.* **14** 765–81
[19] Sims M, Asimakis A, Ariu M and Bradley D D C 2004 *Proc. SPIE* **5519** 59–69
[20] Heliotis G, Bradley D D C, Turnbull G A and Samuel I D W 2002 *Appl. Phys. Lett.* **81** 415–7
[21] Aspnes D E 1980 *J. Opt. Soc. Am.* **70** 1275–7
[22] Campoy Quiles M, Heliotis G, Xia R, Ariu M, Pintani M, Etchegoin P and Bradley D D C 2005 *Adv. Funct. Mater.* **15** 925–33
[23] Campoy Quiles M, Sims M, Zheng K, Hill C, Ariu M, Etchegoin P and Bradley D D C 2005 *Synth. Met.* at press
[24] Ellison C J and Torkelson J M 2002 *J. Polym. Sci.* B **40** 2745–58
[25] Heliotis G, Xia R, Whitehead K S, Turnbull G A, Samuel I D W and Bradley D D C 2003 *Synth. Met.* **139** 727–30
[26] Forrest S R, Bradley D D C and Thompson M E 2003 *Adv. Mater.* **15** 1043–8
[27] Krause S and Lu Z-H 1981 *J. Polym. Sci.* B **19** 1925–8
[28] Beaucage G, Composto R and Stein R S 1993 *J. Polym. Sci.* B **31** 319–26
[29] Kawana S and Jones R A L 2001 *Phys. Rev.* E **63** 021501
[30] Singh L, Ludovice P J and Henderson C L 2004 *Thin Solid Films* **449** 231–41
[31] Kim J H, Jang J and Zin W 2000 *Langmuir* **16** 4064
[32] Forrest J, Dalnoki-Veress K and Dutcher J R 1997 *Phys. Rev.* E **56** 5705–16